



## Research article

# Cardiac endothelial ischemia/reperfusion injury-derived protein damage-associated molecular patterns disrupt the integrity of the endothelial barrier

Sarawut Kumphune<sup>a,b,c</sup>, Pornnthanate Seenak<sup>c,d</sup>, Nitchawat Paiyabhrom<sup>e</sup>,  
Worawat Songjang<sup>c,e</sup>, Panyupa Pankhong<sup>c,e</sup>, Noppadon Jumroon<sup>c,e</sup>,  
Siriwan Thaisakun<sup>f</sup>, Narumon Phaonakrop<sup>f</sup>, Sittiruk Roytrakul<sup>f</sup>,  
Wachirawadee Malakul<sup>g</sup>, Arunya Jiraviriyakul<sup>c,e</sup>, Nitirut Nernpermpisooth<sup>c,d,\*</sup>

<sup>a</sup> Biomedical Engineering and Innovation Research Centre, Chiang Mai University, Muang, Chiang Mai, 50200, Thailand

<sup>b</sup> Biomedical Engineering Institute, Chiang Mai University, Muang, Chiang Mai, 50200, Thailand

<sup>c</sup> Integrative Biomedical Research Unit (IBRU), Faculty of Allied Health Sciences, Naresuan University, Phitsanulok, 65000, Thailand

<sup>d</sup> Department of Cardio-Thoracic Technology, Faculty of Allied Health Sciences, Naresuan University, Phitsanulok, 65000, Thailand

<sup>e</sup> Department of Medical Technology, Faculty of Allied Health Sciences, Naresuan University, Phitsanulok, 65000, Thailand

<sup>f</sup> National Centre for Genetic Engineering and Biotechnology (BIOTEC), National Science and Technology Development Agency, Pathum Thani, 12120, Thailand

<sup>g</sup> Department of Physiology, Faculty of Medical Science, Naresuan University, Phitsanulok, 65000, Thailand

## ARTICLE INFO

**Keywords:**

Cardiac microvascular endothelial cells  
Damage-associated molecular patterns  
Ischemia reperfusion injury  
Endothelial nitric oxide synthase  
Vascular endothelial-cadherin

## ABSTRACT

Human cardiac microvascular endothelial cells (HCMECs) are sensitive to ischemia and vulnerable to damage during reperfusion. The release of damage-associated molecular patterns (DAMPs) during reperfusion induces additional tissue damage. The current study aimed to identify early protein DAMPs in human cardiac microvascular endothelial cells subjected to ischemia-reperfusion injury (IRI) using a proteomic approach and their effect on endothelial cell injury. HCMECs were subjected to 60 min of simulated ischemia and 6 h of reperfusion, which can cause lethal damage. DAMPs in the culture media were subjected to liquid chromatography-tandem mass spectrometry proteomic analysis. The cells were treated with endothelial IRI-derived DAMP medium for 24 h. Endothelial injury was assessed by measuring lactate dehydrogenase activity, morphological features, and the expression of endothelial cadherin, nitric oxide synthase (eNOS), and caveolin-1. The top two upregulated proteins, DNAJ homolog subfamily B member 11 and pyrroline-5-carboxylate reductase 2, are promising and sensitive predictors of cardiac microvascular endothelial damage. HCMECs expose to endothelial IRI-derived DAMP, the lactate dehydrogenase activity was significantly increased compared with the control group ( $10.15 \pm 1.03$  vs  $17.67 \pm 1.19$ , respectively). Following treatment with endothelial IRI-derived DAMPs,

**Abbreviations:** DAMPs, damage-associated molecular patterns; ECs, endothelial cells; eNOS, endothelial nitric oxide synthase; HCMECs, human cardiac microvascular endothelial cells; SI, simulated/ischemia; IRI, ischemia/reperfusion injury; LC-MS/MS, liquid chromatography-tandem mass spectrometry; NOX2, nicotinamide adenine dinucleotide phosphate (NADPH) oxidase 2; PAMPs, pathogen-associated molecular pattern; PGE<sub>2</sub>, prostaglandin E<sub>2</sub>; TC, cells treated with control culture medium; TE, cells treated with endothelial IRI-derived DAMP medium; TGF- $\beta$ , transforming growth factor beta; TLRs, Toll-like receptors; VE-cadherin, vascular endothelial cadherin.

\* Corresponding author. Department of Cardio-Thoracic Technology, Faculty of Allied Health Sciences, Naresuan University, Muang, Phitsanulok, 65000, Thailand.

E-mail address: [nitirutn@nu.ac.th](mailto:nitirutn@nu.ac.th) (N. Nernpermpisooth).

<https://doi.org/10.1016/j.heliyon.2024.e24600>

Received 5 September 2023; Received in revised form 5 January 2024; Accepted 10 January 2024

Available online 17 January 2024

2405-8440/© 2024 The Authors. Published by Elsevier Ltd. This is an open access article under the CC BY-NC-ND license (<http://creativecommons.org/licenses/by-nc-nd/4.0/>).

actin-filament dysregulation, and downregulation of vascular endothelial cadherin, caveolin-1, and eNOS expressions were observed, along with cell death. In conclusion, the early protein DAMPs released during cardiac microvascular endothelial IRI could serve as novel candidate biomarkers for acute myocardial IRI. Distinct features of impaired plasma membrane integrity can help identify therapeutic targets to mitigate the detrimental consequences mediated of endothelial IRI-derived DAMPs.

## 1. Introduction

Reperfusion after coronary occlusion is a standard intervention for salvage of the penumbra region in the acute ischemic myocardium [1,2]. Paradoxically, abrupt restoration of blood flow to the ischemic area can aggravate myocardial and microvascular ischemia/reperfusion injury (IRI) [1,2]. After reopening the occluded infarct-related artery, perfusion to the distal coronary microcirculation is not fully restored despite successful coronary intervention, and microvascular dysfunction can occur after the blockage of the epicardial arteries is relieved [1,3,4]. No reflow or structural microvascular damage is prominent in the impending infarct territory and is highly predictive of adverse clinical outcomes [4]. According to an intricate network of capillaries, coronary microvascular endothelial cells (ECs) are next to cardiomyocytes and are vital for regulating regional microcirculation, capillary exchange, and cell–cell interactions [5,6]. Cardiac ECs regulate the oxygenated blood supply to cardiomyocytes and secrete factors that promote cardiomyocyte function, organization, and survival [5]. Blockage of the main coronary arteries promptly causes oxygen deprivation in the coronary microvasculature and induces coronary microvascular dysfunction that interrupts the blood supply to the heart muscle [3].

Vascular ECs actively participate in immune responses that contribute to a pro-inflammatory milieu and amplify harmful signaling cascades during myocardial IRI [2,7–9]. Endothelial stress or damage can be a major source of critical mediators, including damage-associated molecular patterns (DAMPs), that can directly affect ECs and cells of the neighboring milieu after release [2,6,8,10]. DAMPs and conditional DAMPs are endogenous molecules released passively by membrane rupture due to various types of cell death such as necrosis and apoptosis [9]. Some DAMPs are actively exported to the extracellular space via exocytosis when exposed to stress [2,8,9]. The classical DAMP sensing system includes a series of pathogen-associated molecular patterns (PAMPs), including Toll-like receptors (TLRs), which are expressed in cardiac microvascular ECs [2,8].

Under physiological conditions, cardiac microvascular ECs maintain vascular and myocardial health [6]. On the other hand, during acute myocardial IRI, they lose their protective function and are involved in endogenous oxidative stress and acidosis-induced cytotoxicity, leading to cell damage or death [2,7]. As a consequence of IRI, endothelial DAMPs released from damaged cells can expand damage to viable tissues around the primary infarct site. Currently, there is a lack of specific and effective treatment strategies to limit the damage caused by reperfusion injury. In addition, DAMPs released from cardiac microvascular endothelial IRI have been less intensively investigated in the context of acute myocardial infarction. Therefore, these dynamic cells are attractive targets for post-ischemic myocardial protection, with a particular focus on protein DAMPs that are abundantly generated during reperfusion [6,10].

This study aimed to analyze the proteomic landscape of early protein DAMPs released from human cardiac microvascular ECs subjected to simulated *in vitro* IRI. In addition, we aimed to investigate the impact of endothelial IRI-derived DAMPs on endothelial injury. These findings reveal potential novel biomarker candidates for acute myocardial infarction. The distinct characteristics of human cardiac microvascular endothelial injury may shed light on potential therapeutic strategies to limit damage-associated endothelial IRI-derived DAMPs, ultimately leading to a reduction in the final infarct size.

## 2. Materials and methods

### 2.1. Chemicals and reagents

All the basic chemicals were purchased from Sigma-Aldrich (St. Louis, MO, USA). Phosphate-buffered saline (PBS) tablets were obtained from Gibco (Waltham, MA, USA), and 3-(4,5-dimethyl-2-thiazol)-2,5-diphenyl-2H-tetrazolium bromide (MTT) was purchased from Invitrogen (Carlsbad, CA, USA).

### 2.2. Cell culture

Primary human cardiac microvascular endothelial cells (HCMECs) (C-12285), EC growth medium MV, detachKit, and cryo-SFM were obtained from PromoCell, Inc. (Germany). Cells were cultured in EC growth medium MV without antibiotics or antimycotics and gently detached using a DetachKit. HCMECs at passages 5–7 were maintained in an incubator (37 °C, 5 % CO<sub>2</sub>) until they reached a cell density of approximately 80 % confluency, prior to subsequent experiments.

### 2.3. Simulated ischemia (SI) and IRI

The SI was induced by treatment with a modified Krebs buffer supplemented with 20 mM 2-deoxyglucose, 20 mM sodium lactate,

and 1 mM sodium dithionite at pH 6.5 (ischemic buffer) [11]. In the control group, cells were incubated with modified Krebs buffer supplemented with 20 mM D-glucose and 1 mM sodium pyruvate (control buffer). The cells were cultured in ischemic buffer for 0, 15, 30, 60, and 120 min at 37 °C to optimize the duration of the sublethal injury. For IRI, the cells were cultured in ischemic or control buffer for 60 min and subsequently reperfused with fresh culture medium for 6 h (Fig. 1A). To prepare the control culture medium, the cells were incubated with the control buffer for 60 min, which was then replaced with fresh culture medium for 6 h. Normal HCMECs were subsequently treated with conditioned medium (control medium) for 24 h (TC group). The endothelial IRI-derived DAMP medium was collected after sI with ischemic buffer for 60 min and then reperfused with fresh culture medium for 6 h (endothelial IRI-derived DAMPs medium). Normal HCMECs were treated with endothelial IRI-derived DAMP medium for 24 h (TE group) (Fig. 1B). The control culture and endothelial IRI-derived DAMP media were collected for liquid chromatography-tandem mass spectrometry (LC-MS/MS) analysis. These conditioned media were freshly prepared, and cell debris removal by centrifugation at 5000 g for 5 min at 25 °C and carefully aspirated the supernatant for experiments.

#### 2.4. Cell viability assay

HCMECs were seeded in 96-well plates ( $0.01 \times 10^6$ /well) until 80 % confluence was reached. Cell viability was examined after sI by MTT assay. Briefly, after the removal of the culture medium, 0.01 mg/ml MTT reagent was added and incubated for 4 h at 37 °C. Formazan crystals were dissolved in dimethyl sulfoxide (DMSO), and the absorbance was determined using a microplate spectrophotometer at a wavelength of 570 nm. The percentage cell viability was calculated by comparing the optical density of the sI group with that of the control group (100 % viability).

#### 2.5. Apoptosis assessment by annexin V and propidium iodide (PI) staining

HCMECs were seeded in 6-well plates ( $0.3 \times 10^6$ /well) until 80 % confluence was reached. Dead cells were examined using the Muse Annexin V & Dead Cell Kit (CYTEX®, USA). After inducing sI, IRI, TC, TE, or control, the cells were stained with Annexin V and dead cell reagent (7-AAD) for 20 min before analysis. The assay was performed, and images were acquired utilizing the Muse™ Cell Analyzer from Millipore (MA, USA), following the manufacturer's instructions. The results were presented as the events and percentages of live, apoptotic, and necrotic cells.

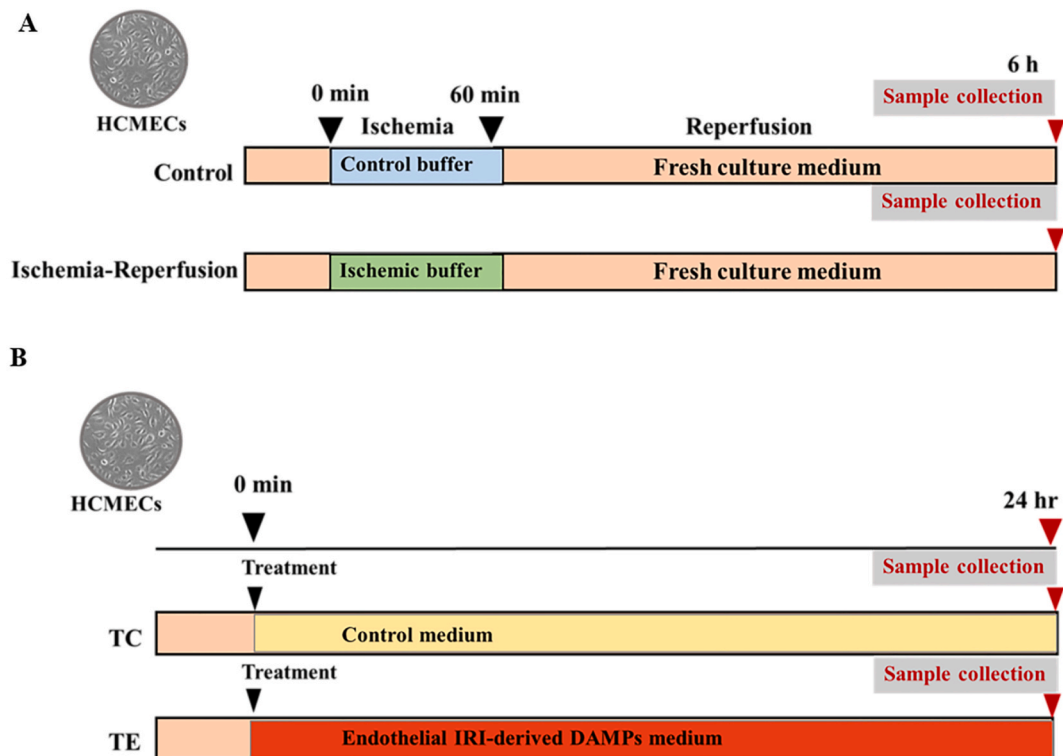


Fig. 1. Experimental Protocols. (A) Simulated IRI Protocol. (B) The endothelial IRI-derived DAMP treatment protocol.

## 2.6. Determination of released-lactate dehydrogenase (LDH) activity

After treating the cells with control medium or endothelial IRI-derived DAMP medium for 24 h, LDH activity in the cell culture medium was measured using a Lactate Dehydrogenase activity assay kit (Sigma-Aldrich, MO, USA). The medium was collected, and cell debris was removed by centrifugation. The conditioned medium (50  $\mu$ l) and master mix reagent (50  $\mu$ l) were added together in a 96-well plate. The mixture was incubated at 37 °C, and the absorbance was measured kinetically at 450 nm after 1 min and 6 min of incubation. The LDH activity was calculated based on the  $\Delta$ 450 value and the standard curve establishment.

## 2.7. Immunofluorescent staining

Immunofluorescence was performed on cells that were plated onto 8-well chamber slides and grown for 48 h before experimental treatment. The culture medium was removed and the cells were fixed, permeabilized, and blocked before staining. The fixed cells were then incubated overnight at 4 °C with phalloidin-iFluor 555 (1  $\mu$ g/ml, ab176756, Abcam, UK), anti-vascular endothelial (VE)-cadherin antibody (1  $\mu$ g/ml, ab33168, Abcam), or anti-caveolin-1 antibody (2  $\mu$ g/ml, ab2910, Abcam) in a dark, moist chamber. This was followed by further incubation at room temperature for 1 h with Alexa Fluor® 488 goat anti-rabbit IgG-H&L, pre-adsorbed at 2  $\mu$ g/ml (ab150085, Abcam). Immunofluorescence images were acquired using a fluorescence microscope with a 20  $\times$  objective lens (MICA MICROHUB, Leica, Germany or ZEISS Apotome 3, Germany).

## 2.8. Western blot analysis

HCMECs were seeded in a T25 flask ( $0.7 \times 10^6$ /well) until 80 % confluence was reached. The cells were treated with the control medium or endothelial IRI-derived DAMP medium for 24 h. The protein was extracted from the cells by adding ice-cold RIPA buffer containing a protease inhibitor and centrifugation at 15,000  $\times$ g for 20 min at 4 °C. The protein concentrations in the supernatants were measured using a bicinchoninic acid protein assay kit (Merck KGaA). Then, 20  $\mu$ g of total protein from cell lysate was separated on 7.5 % sodium dodecyl sulfate-polyacrylamide gel electrophoresis and transferred to polyvinylidene difluoride membranes. The membranes were blocked with 5 % non-fat dry milk for 1 h and then incubated with anti-endothelial nitric oxide synthase (eNOS) at a 1:500 dilution (9572S, Cell Signaling Technology, Inc., Danvers, MA, USA), anti-nicotinamide adenine dinucleotide phosphate (NADPH) oxidase 2 (NOX2) at a 1:500 dilution (ab129068, Abcam, UK), and anti- $\beta$  actin at a 1:5000 dilution (4967S, Cell Signaling Technology, Inc.) at 4 °C overnight. The membranes were then washed with Tris-buffered saline containing Tween-20 (TBST) and incubated with anti-rabbit horseradish peroxidase-conjugated secondary antibody (1:5000) at room temperature for 1 h. Antibody-antigen complexes were visualized by enhanced chemiluminescence using the Luminata Crescendo Western HRP substrate (Merck KGaA). Protein bands were quantified by densitometry using a Bio-Rad image analysis system (Quantity One, Bio-Rad Laboratories, Inc., Hercules, CA, USA) and normalized to  $\beta$ -actin protein expression.

## 2.9. Flow cytometry

HCMECs were cultured in a T25 flask ( $0.7 \times 10^6$ /well) until 80 % confluency. Cells were treated with control medium or endothelial IRI-derived DAMP medium for 24 h and detached with Versine solution (Gibco™, USA). Then,  $5 \times 10^5$  cells were stained with 200  $\mu$ l of 1 % FBS in PBS buffer supplement with anti-caveolin-1 antibody at 2  $\mu$ g/ml (Abcam, ab2910, UK) at 4 °C in the dark for 30 min. To remove the unbound antibody, cells were washed by centrifugation at 1200 rpm in PBS for 5 min at 4 °C, and then they were incubated with Alexa Fluor® 488 goat anti-rabbit IgG-H&L, pre-adsorbed at 2  $\mu$ g/ml (ab150085, Abcam, UK) at 1:1000 dilution for 20 min at 4 °C in the dark. The expression of caveolin-1 in ECs was detected using CytoFlex SRT (Beckman Coulter).

## 2.10. Sample preparation for shotgun proteomics

The control medium and endothelial IRI-derived DAMPs were transferred to a new tube, mixed well with 2 vol of cold acetone, and incubated overnight at -20 °C. The mixture was centrifuged at 10,000  $\times$ g for 15 min and the supernatant was discarded. The pellet was dried and stored at -80 °C prior to use.

## 2.11. In-solution trypsin digestion

The protein concentration of the collected medium was determined by Lowry assay using bovine serum albumin (BSA) as a standard protein [12]. Five micrograms of protein samples were subjected to in-solution digestion. The samples were completely dissolved in 10 mM ammonium bicarbonate (AMBIC). Disulfide bonds were reduced using 5 mM dithiothreitol (DTT) in a 10 mM AMBIC at 60 °C for 1 h, and alkylation of sulfhydryl groups was achieved using 15 mM Iodoacetamide (IAA) in 10 mM AMBIC at room temperature for 45 min in the dark. The protein samples were digested with sequencing-grade porcine trypsin (1:20 ratio) for 16 h at 37 °C. Tryptic peptides were dried using a speed vacuum concentrator and resuspended in 0.1 % formic acid for liquid chromatography-tandem mass spectrometry (LC-MS/MS) analysis.

## 2.12. Liquid chromatography with tandem mass spectrometry (LC-MS-MS)

Identification of protein by LC/MS-MS was previously describe in the previous publication [13]. Tryptic peptide samples were prepared for injection into an Ultimate 3000 Nano/Capillary LC System (Thermo Scientific) coupled with a ZenoTOF 7600 mass spectrometer (SCIEX, Framingham, MA, USA). Briefly, 1  $\mu$ l of digested peptide was enriched on a  $\mu$ -Precolumn with dimensions of 300  $\mu$ m inner diameter (i.d.)  $\times$  5 mm length, packed with C18 Pepmap 100, 5  $\mu$ m, and 100  $\text{\AA}$  particles (Thermo Scientific). The enriched peptides were then separated on a 75  $\mu$ m i.d.  $\times$  15 cm length analytical column, packed with Acclaim PepMap RSLC C18, 2  $\mu$ m, 100  $\text{\AA}$  particles, equipped with a nanoViper fitting (Thermo Scientific). The C18 column was placed in a thermostat column at 60  $^{\circ}$ C in an oven. Solvent A and B containing 0.1 % formic acid in water and 0.1 % formic acid in 80 % acetonitrile, respectively, were supplied to the analytical column. A gradient of 5–55 % solvent B was used to elute the peptides at a constant flow rate of 0.30  $\mu$ l/min for 30 min.

The source and gas parameters on the ZenoTOF 7600 system for all acquisitions were as follows: the ion source gas 1 was set to 8 psi, the curtain gas was set to 35 psi, the CAD gas was set to 7 psi, the source temperature was set to 200  $^{\circ}$ C, the polarity was set to positive, and the spray voltage was set to 3300 V. The DDA method was used to select the 50 most abundant precursor ions per survey MS1 for MS/MS at a minimum intensity threshold of 150 counts per second (cps). The sampled precursor ions were dynamically excluded for 12 s after two MS/MS samplings. This dynamic exclusion was implemented while performing MS/MS sampling using the dynamic collision energy. The MS2 spectra were collected from 100 to 1800  $m/z$  with a 50 ms accumulation time and the Zeno trap enabled. For the collision energy equation, the declustering potential was set to 80 V with a 0 V DP spread, and the CE spread was set to 0 V. The time bins to sum were set to eight, with all channels enabled and a 150,000 cps Zeno trap threshold. The cycle time for the top 60 DDA method was 3.0 s.

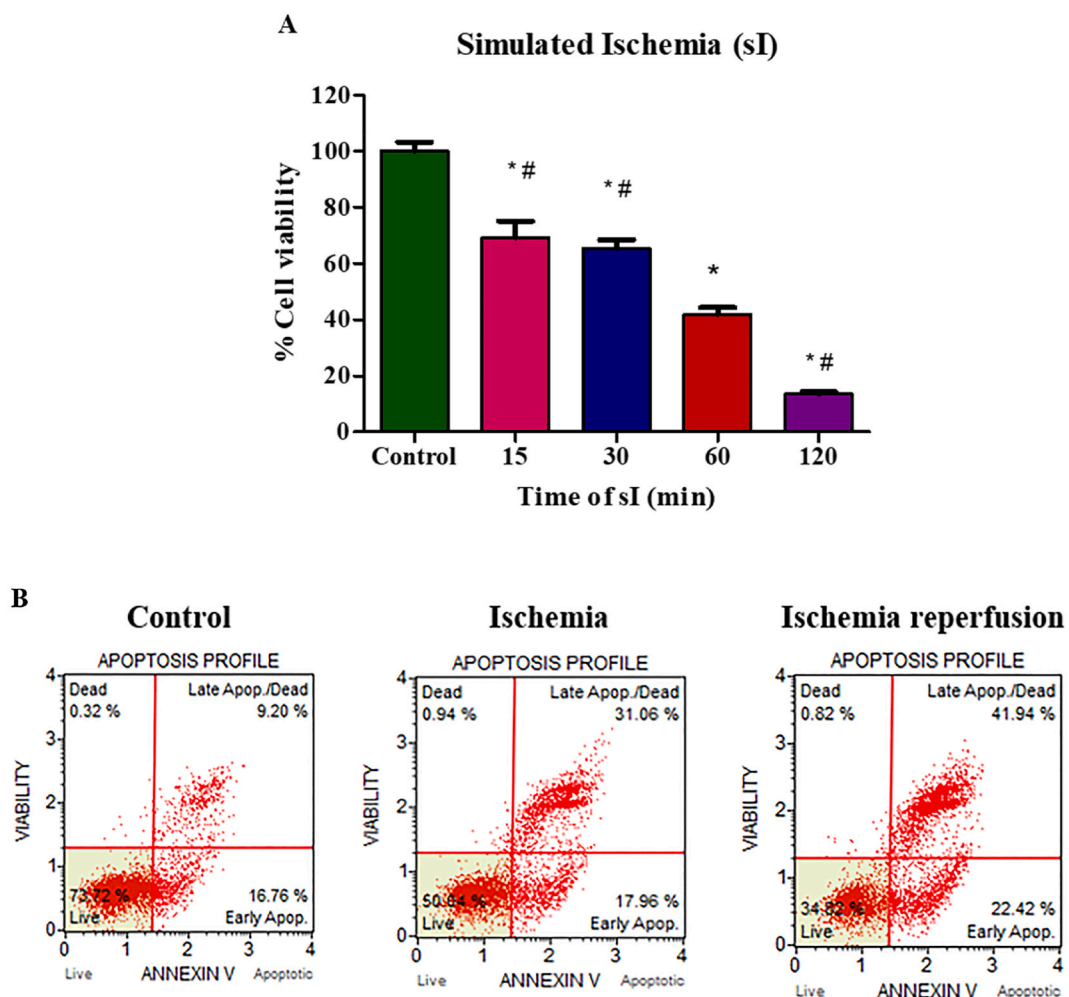


**Fig. 2.** Optimization of the simulated IRI. (A) Viability of HCEMCs subjected to sI treatment for 0, 15, 30, 60, or 120 min. Graphical representation of data from three independent experiments performed in duplicates. Values are expressed as mean  $\pm$  SEM. (B) Different types of cell death using Annexin V and propidium iodide staining in the control, ischemic, or ischemia/reperfusion groups of two experiments with independent cell preparations. \* $p < 0.05$  vs control, # $p < 0.05$  vs sI at 60 min.

### 2.13. Bioinformatics and data analysis

MaxQuant 2.2.0.0 was used to quantify the proteins in individual samples using the Andromeda search engine to correlate MS/MS spectra with the UniProt *Homo sapiens* database. Label-free quantitation with MaxQuant's standard settings was performed: a maximum of two missed cleavages, mass tolerance of 0.6 Da for the main search, trypsin as the digesting enzyme, carbamidomethylation of cysteine as the fixed modification, and oxidation of methionine and acetylation of the protein N-terminus as variable modifications. Only peptides with a minimum of 7 amino acids and at least one unique peptide, were required for protein identification. Only proteins with at least two peptides and one unique peptide were considered as being identified and used for further data analysis. The protein false discovery rate (FDR) was set at 1 % and was estimated using reverse search sequences. The maximum number of modifications per peptide was set to five. The proteins present in the *Homo sapiens* proteome were downloaded from UniProt as search FASTA files. Additionally, the software automatically included potential contaminants present in the "contaminants.fast" file that comes with Macquet in the search space.

### 2.14. Proteomics data analysis

The MaxQuant "ProteinGroups.txt" file was loaded into Perseus version 1.6.6.0, and potential contaminants that did not correspond to any UPS1 protein were removed from the data and transformed into log base 2. Missing values were imputed in Perseus using a constant value (zero). Statistical analysis and visualization were conducted using Metaboanalyst 5.0 [14,15]. STITCH 5.0 was used to predict the functional interaction networks between the identified proteins and small molecules [16].

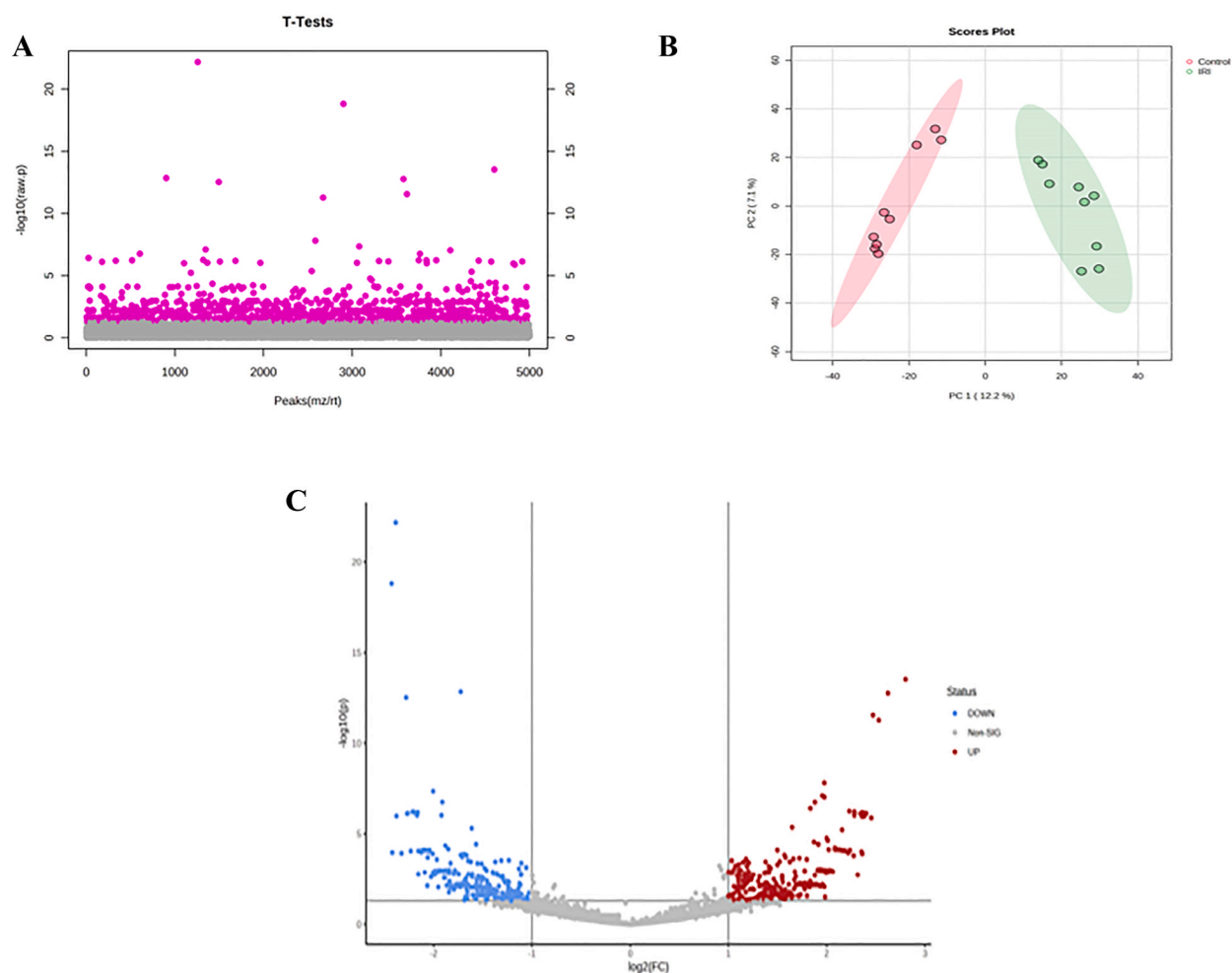


**Fig. 3.** Identification of specific proteins in human cardiac microvascular endothelial IRI media. (A) A total of 762 proteins in the IRI group were significantly different from those in the control group, as determined using a *t*-test. (B) PCA was performed for dimensional dataset reduction in the IRI and control groups to demonstrate group discrimination. (C) Volcano plot of the IRI simulation shows 352 significantly upregulated proteins and 364 downregulated proteins.

## 2.15. Statistical analysis

All values are expressed as the mean  $\pm$  standard error of the mean (SEM). Differences between the TC and TE groups were assessed using an unpaired *t*-test. Ischemia/reperfusion studies were compared among groups using one-way analysis of variance (ANOVA) with post hoc multiple comparisons using the Tukey–Kramer test. All statistical analyses were performed using GraphPad Prism version 5 (GraphPad Software Inc., San Diego, CA, USA). A *p*-value of less than 0.05 indicated a statistically significant difference.

## 3. Results

### 3.1. Optimization of sI

sI reduces HCMEC viability in a time-dependent manner. After 15 min of incubation with the ischemic buffer, an initial loss of cell viability was observed. After 15, 30, 60, and 90 min of sI, the cell viability was significantly decreased to  $69.21 \pm 5.90$  %,  $65.39 \pm 3.02$  %,  $41.90 \pm 2.43$  %, and  $13.52 \pm 0.81$  % vs 100 %, respectively, compared with control conditions (Fig. 2A). In the subsequent IRI experiment, an ischemic duration of 60 min was used, which resulted in an optimal lethal injury close to a 50 % cell death rate. Both sI and IRI significantly increased the total cell death of HCMECs compared to the control group ( $23.06 \pm 2.9$  %,  $46.39 \pm 2.63$  %,  $68.63 \pm 4.27$ , respectively). A significant increase in cell death and severity of cellular damage was observed under ischemia/reperfusion conditions compared to that under ischemic conditions. Specifically, many cells exhibited late apoptosis, dead cells, and debris (Fig. 2B). These results indicate that sI for 60 min followed by reperfusion for 6 h can cause lethal damage and cell death in HCMECs; thus, this protocol could be an appropriate setting for studying IRI.

### 3.2. Identification of cardiac microvascular EC-specific protein DAMPs in the IRI simulation

After IRI, the secreted cell culture media were collected for proteomic analysis using the shotgun proteomic method. A total of 7513 differentially expressed proteins (features) were identified between the IRI and control groups in the media. To analyze the differences in individual values from the mean values of the groups, a *t*-test analysis of the data was performed. The results showed that the expression of 762 proteins was significantly different from that in the control group (Fig. 3A). Principal component analysis (PCA) and partial least squares-discriminant analysis (PLS-DA) were performed to evaluate protein alterations and determine the discrimination of the dataset. Pattern recognition techniques, including PCA and PLS-DA, were applied to the dataset to directly evaluate the induced protein alterations and determine whether differences in proteomic profiles existed among the groups. The scores were plotted to depict the data and samples with similar proteomic profiles tended to congregate into one section of the plot. The control and IRI groups were distinguished from each other and from the other ischemia groups, as shown by the two-dimensional score plots of the PCA (PC1:12.1 %, PC2:7.1 %) and PLS-DA (PC1:12.1 %, PC2:6.7 %) models (Fig. 3B and C).

### 3.3. Identification of candidate proteins for novel IRI biomarkers of cardiac microvascular ECs

The volcano plot (Fig. 3C) shows the expressed proteins with adjusted significance values below the alpha level of 0.05, and two-fold changes were considered significant. In the IRI group, 352 proteins were significantly upregulated compared to those in the control group. The top 20 upregulated proteins were identified using volcano plots.

**Table 1**

List of the top 20 candidate proteins that were upregulated upon IRI stimulation.

Protein names	f.value	p.value	-log10p	FDR
DnaJ homolog subfamily B member 11 (APOBEC1-binding protein 2) (HSP40)	6.9755	2.8023	2.91E-14	13.536
Pyroline-5-carboxylate reductase 2 (P5C reductase 2) (P5CR 2) (EC 1.5.1.2)	6.1601	2.623	1.69E-13	12.771
Cytochrome c oxidase subunit 8C	5.777	2.5303	5.23E-12	11.281
Polypeptide N-acetylgalactosaminyltransferase 14 (EC 2.4.1.41)	5.5453	2.4713	2.75E-12	11.561
TRAF3-interacting JNK-activating modulator (TRAF3-interacting protein 3)	5.4788	2.4539	1.31E-06	5.8827
Ubiquitin carboxyl-terminal hydrolase 15 (EC 3.4.19.12)	5.2838	2.4016	7.38E-07	6.1319
Retinoblastoma-like protein 1 (p107) (pRb1)	5.2196	2.3839	1.02E-06	5.9906
A-kinase anchor protein 6 (AKAP-6)	5.1494	2.3644	6.51E-07	6.1862
Splicing factor, arginine/serine-rich 19	5.1403	2.3618	0.000123	3.9094
BLOC-2 complex member HPS5 (Alpha-integrin-binding protein 63)	5.1388	2.3614	1.09E-06	5.9633
CMT1A duplicated region transcript 15 protein-like protein	5.1305	2.3591	7.87E-07	6.104
Gamma-adducin (Adducin-like protein 70)	5.1186	2.3558	9.65E-05	4.0153
Storkhead-box protein 2	5.0802	2.3449	7.55E-07	6.1221
Inhibitor of Bruton tyrosine kinase (IBtk)	4.9792	2.3159	0.001808	2.7428
Interferon-induced protein 44 (p44) (Microtubule-associated protein 44)	4.8715	2.2844	6.74E-07	6.1715
Gamma-glutamylaminocyclotransferase (GGACT) (EC 4.3.2.8)	4.8629	2.2818	5.91E-07	6.2285
Testis-specific Y-encoded-like protein 6 (TSPY-like protein 6)	4.8616	2.2814	9.38E-07	6.0278
Glucosylceramide transporter ABCA12 (EC 7.6.2.1)	4.8386	2.2746	0.00016	3.7954
Protein phosphatase 1 regulatory subunit 3E	4.71	2.2357	8.04E-05	4.0945
Zinc finger protein 165	4.6914	2.23	5.56E-07	6.255

The potential interactions of the top 20 selected proteins (Table 1) were analyzed using STITCH 5.0, a web-based resource for predicting the interactions between proteins and small molecules. The analysis revealed that among the top 20 proteins, 17 interacted with other proteins (Fig. 4A). Additionally, of the 20 candidate proteins, 7 interacted with 2 other proteins. The analysis also predicted a signaling pathway related to the transforming growth factor-beta receptor signaling pathway (GO: 0007179, FDR = 4.45e-09) (Fig. 4B).

### 3.3.1. Cardiac microvascular endothelial IRI-derived DAMPs mediate endothelial plasma membrane disruption

HCMECs treated with endothelial IRI-derived DAMP medium showed significantly increased LDH activity compared to those treated with the control medium ( $10.15 \pm 1.03$  vs  $17.67 \pm 1.19$ ) (Fig. 5A). These data suggested that exposure to endothelial IRI-derived DAMPs for 24 h activated the release of LDH into the culture medium, which may be a good indicator of cellular damage. The cells showed significant alterations in size, shape, and cytoskeletal arrangement 24 h after treatment with the endothelial IRI-derived DAMP medium. Cell morphology exhibited boundary area changes, with actin filaments contracting and elongating, and a loss of their polygonal-shaped phenotype, indicating cell boundary deformation (Fig. 5C). Additionally, the expression of VE-cadherin, a major endothelial adhesion molecule located at junctions between ECs, was reduced in response to IRI-derived DAMP treatment (Fig. 5D). TE also induced significant cell death ( $19.95 \pm 1.29$  vs  $34.13 \pm 0.62$ ) (Fig. 5B). This suggests that the detrimental effects of endothelial IRI-derived DAMPs have a major impact on plasma membrane integrity and cause multiple cellular disruptions before the cell death occurs.

### 3.4. Endothelial IRI-derived DAMPs suppressed eNOS and caveolin-1 expression

A significant reduction in eNOS expression was observed after 24 h of treatment with endothelial IRI-derived DAMP medium compared with control culture medium ( $1.12 \pm 0.04$  vs  $0.73 \pm 0.03$ ) (Fig. 6A). In contrast, NOX2 expression was significantly increased after stimulation with endothelial IRI-derived DAMPs compared to that in the control ( $1.02 \pm 0.05$  vs  $1.39 \pm 0.07$ ) (Fig. 6A). The expression of caveolin-1 in the plasma membrane was disrupted after culturing in endothelial IRI-derived DAMP medium (Fig. 6B). Expression levels were reduced by approximately half (Fig. 6C).

## 4. Discussion

Paradoxically, IRI aggravated cellular dysfunction and death. In the present study, acute IRI induced lethal cardiac microvascular endothelial damage. Activated endothelial IRI induces release of numerous protein-associated DAMPs. Endothelial IRI-derived DAMPs aggravate endothelial barrier disruption and suppress the main eNOS regulatory protein, caveolin-1, indicating cellular endothelial injury and dysfunction.

The release of DAMPs from the infarcted myocardium has been extensively studied while limit information of cardiac microvascular endothelial DAMPs during IRI [2,17–19]. ECs are highlighted in immunology studies because they are sources of different types

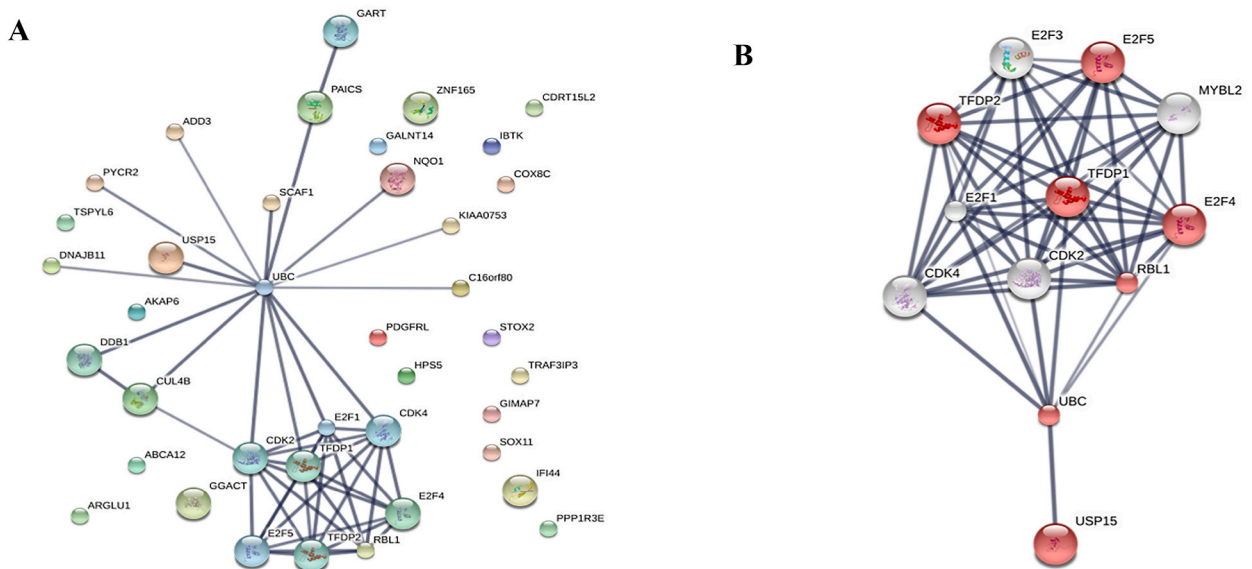


**Fig. 4.** Identification of candidate proteins as novel biomarkers of human cardiac microvascular endothelial IRI biomarkers. (A) Potential interactions between 20 candidate proteins were analyzed using STITCH 5.0. (B) Prediction of protein interactions involving the transforming growth factor-beta receptor signaling pathway, which hit two candidate proteins: ubiquitin carboxyl-terminal hydrolase 15 (EC 3.4.19.12) and retinoblastoma-like protein 1 (p107) (pRb1) (B).

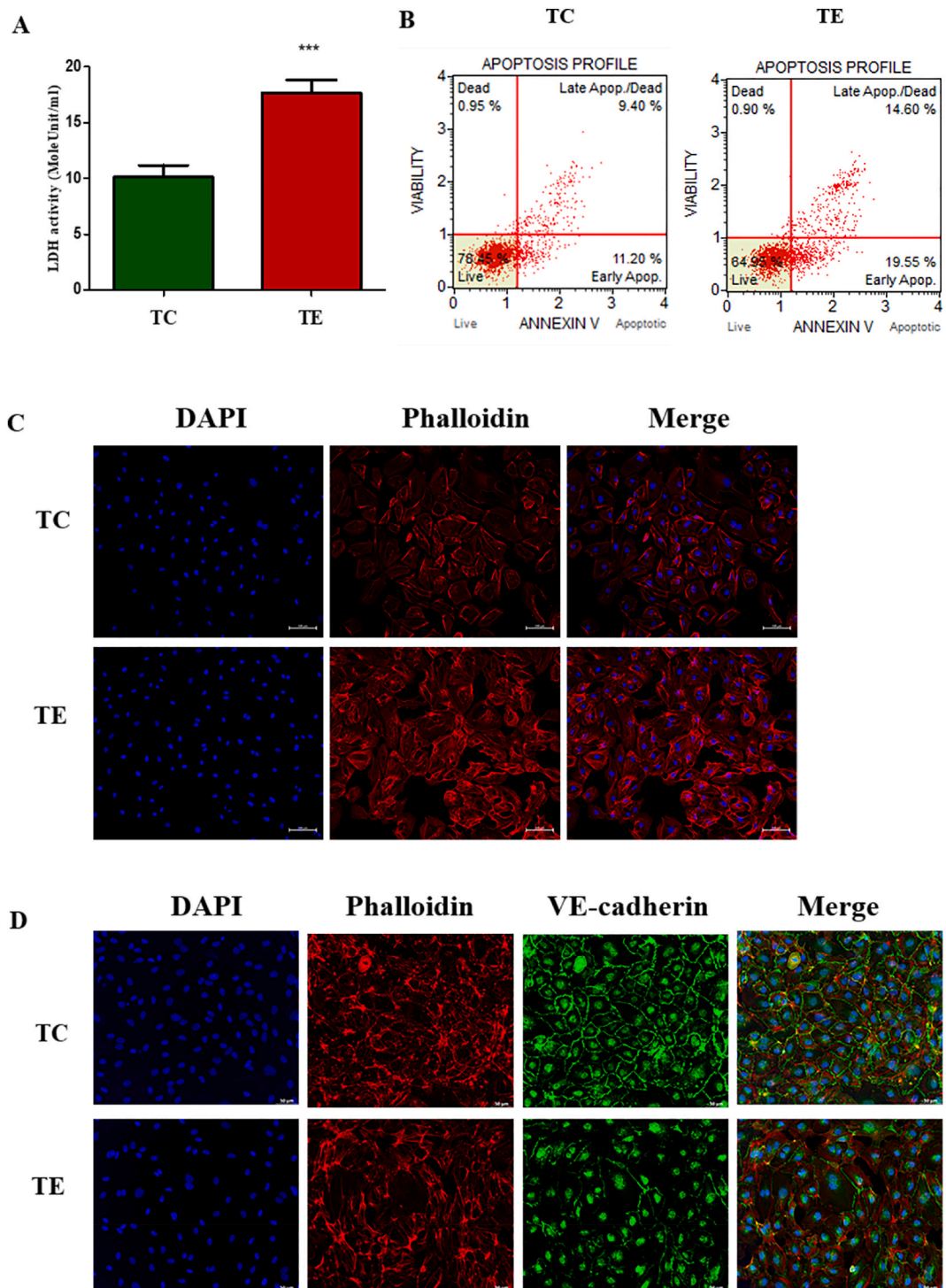
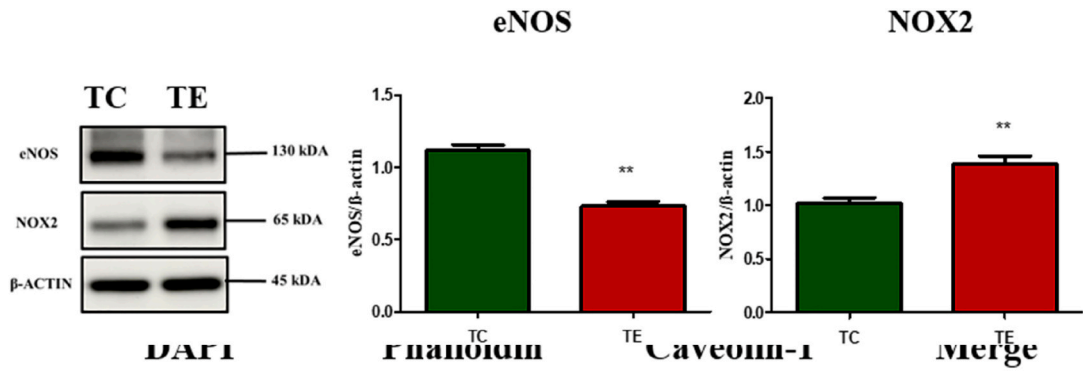
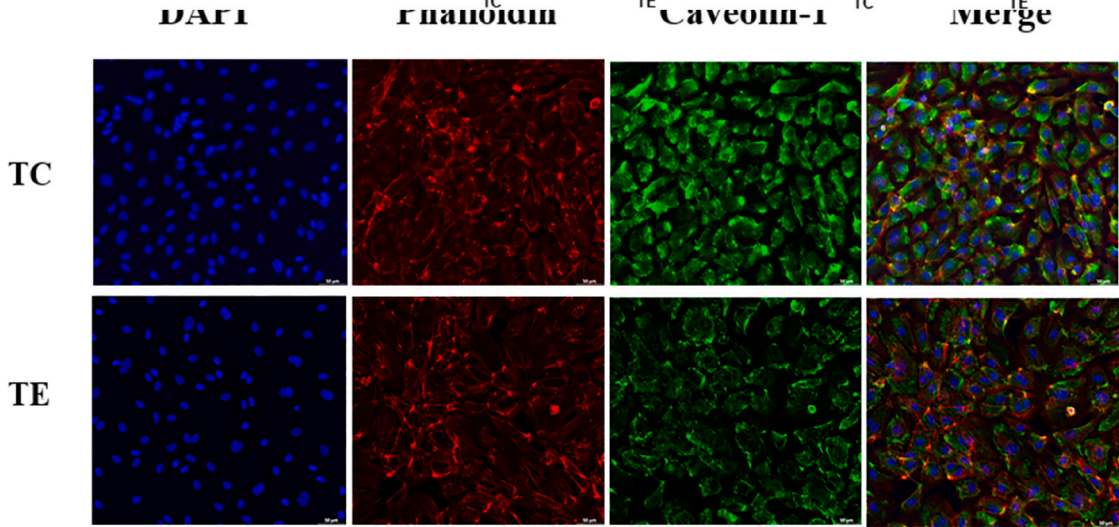


**Fig. 5.** Endothelial IRI-derived DAMPs mediate endothelial plasma membrane disruption. (A) LHD activity in the media of cells treated with control culture medium (TC) or endothelial IRI-derived DAMP medium (TE). Graphical representation of the data from six independent experiments performed in duplicate. Values are expressed as mean  $\pm$  SEM. (B) The different types of cell death using Annexin V and propidium iodide staining in the TC and TE groups of three experiments with independent cell preparations (C) Cellular morphology of endothelial cells of TC and TE groups. Cells were labeled with phalloidin-actin filaments (red) and DAPI-nuclei (blue) in three independent experiments. (D) VE-cadherin expression (green) in the endothelial cells of the TC and TE groups from three independent experiments.  $***p < 0.0001$  vs TC. (For interpretation of the references to colour in this figure legend, the reader is referred to the Web version of this article.)

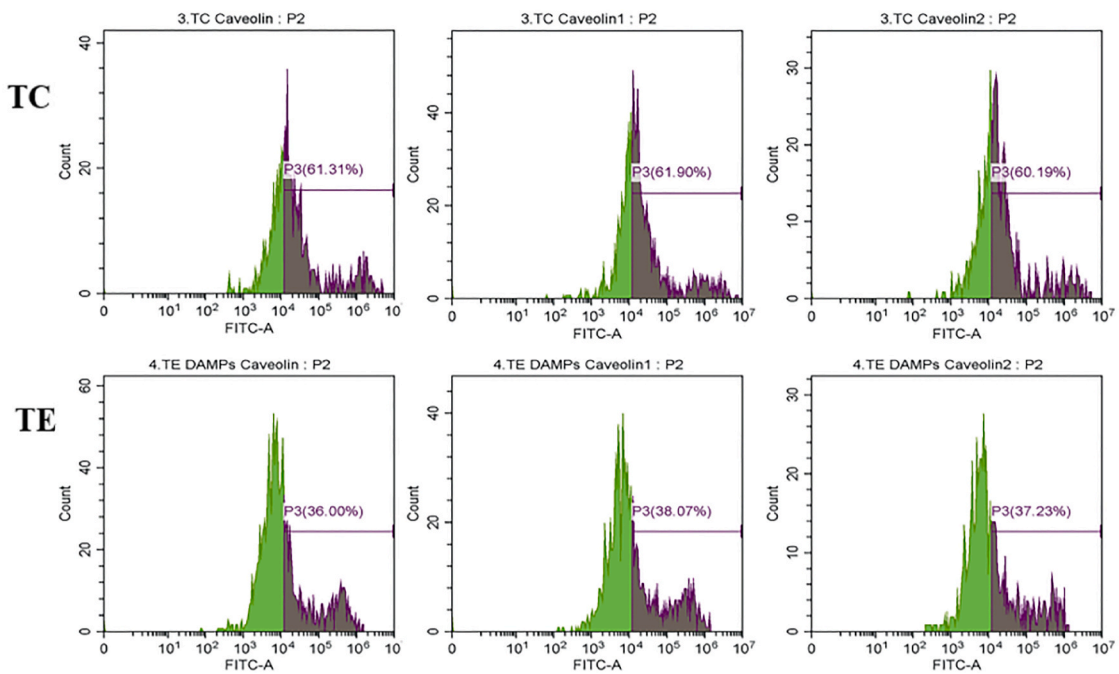
**A**



**B**



**C**



(caption on next page)

**Fig. 6.** Endothelial IRI-derived DAMPs suppress eNOS and caveolin-1 expression levels. (A) Representative eNOS and NOX2 expression levels in PDVF membranes were determined by Western blot analysis (Supplementary Fig. 6A). Graphical representation of data from five experiments with independent cell preparations. Values are expressed as mean  $\pm$  SEM. (B) Caveolin-1 expression (green) in the endothelial cells of the TC and TE groups from three independent experiments. (C) Flow cytometry histogram plots of the percentage of cells positive for caveolin-1 in the TC and TE groups from three independent experiments.  $**p < 0.01$  vs TC. (For interpretation of the references to colour in this figure legend, the reader is referred to the Web version of this article.)

of DAMPs panels and express DAMP-sensing receptors, including Toll-like receptors (TLRs), NOD-like receptors (NLRs), and receptors for advanced glycation end products (RAGE) on the plasma membrane [2,17–19]. Current medical strategies for detecting and monitoring cardiac microvascular injury in patients with obstructive coronary artery disease or in those who have undergone revascularization but experience persistent symptoms of chest pain are inadequate [20]. ECs are sensitive to both ischemia and reperfusion, and damage starts from the ECs of the small coronary arteries and spreads to the surrounding cardiomyocytes [21]. After 5–60 min of reperfusion, ECs appear to be the targets of lethal injury. However, after 2 h of reperfusion, a significant increase in cardiomyocyte death [21]. This time-series pattern presents an opportunity for early detection and rapid intervention to prevent life-threatening complications, particularly by focusing on emerging candidate proteins of endothelial origin, as opposed to currently used cardiac biomarkers. However, the recovery of endothelial cells from ischemia can result in the secretion of protective physiological factors that differ from those released by injured or dead cells. IRI interrupts autocrine or paracrine factors including cytokines, chemokines and growth factors are interrupted by IRI [22]. Hence, single-cell analysis with a fine-tuned design could unveil concealed protein-DAMPs of some individual physiological or pathological patterns and provide more therapeutic approaches. Therefore, it is necessary to identify novel IRI biomarkers in cardiac microvascular ECs. The top 2 upregulated proteins, DNAJ homolog subfamily B member 11 (HSP40) and pyrroline-5-carboxylate reductase 2 (PYCR2), are promising candidate biomarkers for predicting cardiac microvascular endothelial damage. The prediction of potential interactions of 2 from the top 20 candidate proteins was related to the transforming growth factor-beta (TGF- $\beta$ ) signaling pathway. TGF- $\beta$  is a multifunctional cytokine that plays a critical role in many physiological and pathological processes. During IRI, TGF- $\beta$  has been shown to be a protective mediator during the initial phase of inflammatory mediated injury through its actions on the endothelium [23]. On the contrary, TGF- $\beta$  can contribute to apoptotic cell death in cardiomyocytes of adult rats through TGF- $\beta$ -SMAD-signaling pathways [24]. Cardiac ECs are also identified as sources of TGF- $\beta$ , and free oxygen radicals are known to induce TGF- $\beta$  activation [24]. Owing to a multifaceted response of TGF- $\beta$  activation, the interaction of acute endothelial IRI-derived DAMPs and downstream TGF- $\beta$  apoptotic signaling requires further investigation [25].

Our study introduces the novel conceptual idea that the application of total DAMPs is more realistic in reflecting actual situations than a single common DAMP approach. This introduces a potential explanation for the failure of the latter approach to translate into clinical practice. By profiling endothelial IRI-derived DAMPs and identifying their prognostic role, we can guide the selection of prospective therapies that focus on endothelial approaches to minimize serious outcomes. Currently, clear strategic treatments for cardiac microvascular endothelial injury and dysfunction are lacking. The current interventions for cardiac microvascular dysfunction, including angiotensin-converting enzyme inhibitors and L-arginine, primarily aim to alleviate ischemic damage [20]. Approaching cardiac microvascular ECs damage and dysfunctions are challenge and can be a successful point to alleviate the additional myocardial injury during reperfusion.

Microvascular destruction and capillary leakage play crucial roles in determining the extent of injury to the affected microcirculatory territory, leading to significant myocardial edema and intramyocardial hemorrhage during both the initial and late phases of reperfusion [1,26]. LDH is found in the cytosol and rapidly released into the extracellular space upon damage to the plasma membrane [27]. Elevated LDH activity reflects the abnormal vascular permeability induced by endothelial IRI-derived DAMPs, which are the predominant factors leading to capillary leakage in the myocardium affected by IRI. VE-cadherin is an essential component of the adherens junction [28]. The lowest VE-cadherin levels were observed in the no-reflow region of the infarcted myocardium [29]. In the plasma membrane, the endothelial barrier is stabilized by the attachment of VE-cadherin to thick cortical bands of the actin cytoskeleton [26]. In response to exogenous danger signals, the cytoskeleton is deformed due to the contraction and elongation of actin filaments, which is indicative of transcellular fiber stress. If these are coincident with the homotypic complexes of VE-cadherin disruption, it could lead to the opening of the adherens junction and, consequently, dramatically increase vascular permeability [26]. The destructive morphological features of suppressed VE-cadherin expression and cell–cell boundary deformations, were demonstrated in HCMECs after endothelial IRI-derived DAMP treatment. These results suggest that endothelial IRI-derived DAMPs can directly aggravate the damage to ECs and play a key role in excessive vascular permeability, thereby mediating capillary leakage after IRI. Currently, there is a lack of strategic clarity to inhibit the DAMPs pathway during IRI; however, in immunogenic tumor cell death with gemcitabine chemotherapy, prostaglandin E<sub>2</sub> (PGE<sub>2</sub>) was introduced as an inhibitory DAMPs, which functions as an immunosuppressive counterpoise of adjuvant DAMPs [30]. Therefore, to generating idea blocking the effect of DAMPs on normal HCMECs by pretreatment with PGE<sub>2</sub> before exposure to DAMPs is challenging. Moreover, several DAMPs inhibitor have been studied that could provide therapeutic effects. However, the effect of inhibitory DAMPs on vascular endothelial cells subjected to IRI has not been investigated.

Cardiac microvascular dysfunction or no-reflow, is considered evidence of post-myocardial ischemia. The caveolae play a vital role in protecting ECs from membrane rupture, stabilizing eNOS expression and regulating its activity, whereas eNOS-derived nitric oxide promotes caveolae-mediated endocytosis [31,32]. The scaffold protein caveolin-1 plays a pivotal role in caveolae formation and eNOS is highly expressed in caveolae of plasma membrane [31,32]. Therefore, the disruption of caveolin-1 affects eNOS signaling [33]. Depletion of caveolin-1 and/or eNOS may be linked to vascular complications including capillary rupture [31,32]. Thus, reciprocal

regulation of eNOS and caveolin-1 interactions is of paramount importance [33]. Constitutive nitric oxide (NO) produced by eNOS in cardiac microvascular ECs plays a vital role in the regulation of microcirculation and antioxidant properties [34]. Hence, maintaining the normal expression of eNOS and subsequent NO production with a focus on its role seems to provide superior protection during IRI [35]. NOX2 is a major source of superoxide ( $O_2^-$ ) and hydrogen peroxide ( $H_2O_2$ ), and is upregulated in response to IRI [36]. Therefore, oxidative stress after reperfusion may be partially mediated by NOX2 upregulation following the release of endothelial IRI-derived DAMPs. Normally, NOX2 produces  $O_2^-$ , which is converted to stable  $H_2O_2$  [37]. Therefore, the increased level of NOX2 observed in this study likely contributed to the decreased eNOS expression in ECs [38]. According to our findings, the disruption of caveolin-1, eNOS, and NOX2 expression may provide a potential clue for recovering endothelial homeostasis after IRI. Based on our findings, leakage of HSP40 indicated ER stress and ER stress has been reported to activate the NLRP3 inflammasome as well as upregulate NOX2 expression, actin stress fiber formation, or VE-cadherin disruption could be a downstream effector of NLRP3 inflammasome activation. Therefore, the potential cascade that promotes the development of endothelial dysfunction by DAMPs could be a driver of the TLR4/NLRP3 signaling pathway [39]. In addition, the loss of a crucial co-chaperone HSP40 interaction with the HSP70 family in the cytoplasmic compartment and lowering of the mitochondrial enzyme PYCR2 level to promote aerobic glycolysis can cause cellular unfolded protein response abnormalities, and interrupt normal aerobic glycolysis, respectively, which aggravate the ECs to a lethal threat [40,41]. Preserving the functional roles of the endothelium in regulating the vascular tone, facilitating adequate blood flow to meet myocardial demands, and maintaining membrane integrity and permeability are crucial. Exploring the use of protective exogenous nitric oxide supplementation is essential in this regard [42]. Additionally, focusing on the interaction between eNOS and caveolin-1 could be a promising next step in alleviating the additional endothelial dysfunction resulting from the release of DAMPs during IRI.

## 5. Conclusion

This study demonstrated that primary human cardiac microvascular ECs release numerous DAMP-associated proteins during simulated IRI and have a detrimental impact on endothelial plasma membrane integrity. Further analysis of these specific DAMPs and their biological functions may reveal novel candidate biomarkers and potential therapeutic targets for coronary artery disease.

## Data availability statement section

The data will be made available upon request.

## Ethics Declarations

The study was reviewed and approved by the Naresuan University Institutional Biosafety Committee (approval number: NUIBC OT 64-11-51).

## CRedit authorship contribution statement

**Sarawut Kumphune:** Writing – review & editing, Writing – original draft, Validation, Methodology, Investigation, Funding acquisition, Formal analysis, Data curation, Conceptualization. **Pornthanate Seenak:** Validation, Methodology, Formal analysis, Data curation. **Nitchawat Paiyabhrom:** Writing – original draft, Validation, Methodology, Formal analysis, Data curation. **Worawat Songiang:** Validation, Methodology, Formal analysis, Data curation. **Panyupa Pankhong:** Methodology, Formal analysis, Data curation. **Noppadon Jumroon:** Writing – original draft, Formal analysis. **Siriwan Thaisakun:** Validation, Formal analysis, Data curation. **Narumon Phaonakrop:** Validation, Formal analysis, Data curation. **Sittiruk Roytrakul:** Validation, Methodology, Formal analysis, Data curation. **Wachirawadee Malakul:** Validation, Methodology, Formal analysis, Data curation, Conceptualization. **Arunya Jiraviriyakul:** Methodology, Investigation, Funding acquisition, Data curation, Conceptualization. **Nitirut Nernpermpisooth:** Writing – review & editing, Writing – original draft, Supervision, Methodology, Investigation, Funding acquisition, Formal analysis, Data curation, Conceptualization.

## Declaration of competing interest

The authors declare that they have no known competing financial interests or personal relationships that could have appeared to influence the work reported in this paper.

## Acknowledgements

This study was supported by Naresuan University, Thailand and the National Science, Research, and Innovation Fund (NSRF) (grant number: R2565B088) for N.N. and A.J. Research facilities and equipment were supported by the Integrative Biomedical Research Unit (IBRU), Faculty of Allied Health Sciences, Naresuan University, Thailand and this study was partially supported by Chiang Mai University, Thailand through Biomedical Engineering and Innovation Research Center, Chiang Mai University, Thailand. We would like to thank Editage ([www.editage.com](http://www.editage.com)) for the English language editing.

## Appendix A. Supplementary data

Supplementary data to this article can be found online at <https://doi.org/10.1016/j.heliyon.2024.e24600>.

## References

- [1] M. Sezer, N. van Royen, B. Umman, Z. Bugra, H. Bulluck, D.J. Hausenloy, S. Umman, Coronary microvascular injury in reperfused acute myocardial infarction: a view from an integrative perspective, *J. Am. Heart Assoc.* 7 (21) (2018) e009949.
- [2] M.J.M. Silvis, S.E. Kaffka, Genaamd Dengler, C.A. Odille, M. Mishra, N.P. van der Kaaij, P.A. Doevendans, J.P.G. Sluijter, D.P.V. de Kleijn, S.C.A. de Jager, L. Bosch, G.P.J. van Hout, Damage-associated molecular patterns in myocardial infarction and heart transplantation: the road to translational success, *Front. Immunol.* 11 (2020) 599511.
- [3] J. Wei, S. Cheng, C.N. Bairey Merz, Coronary microvascular dysfunction causing cardiac ischemia in women, *JAMA* 322 (23) (2019) 2334–2335.
- [4] L.S.F. Konijnenberg, P. Damman, D.J. Duncker, R.A. Kloner, R. Nijveldt, R.M. van Geuns, C. Berry, N.P. Riksen, J. Escaned, N. van Royen, Pathophysiology and diagnosis of coronary microvascular dysfunction in ST-elevation myocardial infarction, *Cardiovasc. Res.* 116 (4) (2020) 787–805.
- [5] P.C. Hsieh, M.E. Davis, L.K. Lisowski, R.T. Lee, Endothelial-cardiomyocyte interactions in cardiac development and repair, *Annu. Rev. Physiol.* 68 (2006) 51–66.
- [6] A.K. Singhal, J.D. Symons, S. Boudina, B. Jaishy, Y.T. Shiu, Role of endothelial cells in myocardial ischemia-reperfusion injury, *Vasc. Dis. Prev.* 7 (2010) 1–14.
- [7] A. Frank, M. Bonney, S. Bonney, L. Weitzel, M. Koeppen, T. Eckle, Myocardial ischemia reperfusion injury: from basic science to clinical bedside, *Semin. CardioThorac. Vasc. Anesth.* 16 (3) (2012) 123–132.
- [8] Y. Shao, J. Saredy, W.Y. Yang, Y. Sun, Y. Lu, F. Saaoud, C. Drummer, C. Johnson, K. Xu, X. Jiang, H. Wang, X. Yang, Vascular endothelial cells and innate immunity, *Arterioscler. Thromb. Vasc. Biol.* 40 (6) (2020) e138–e152.
- [9] A. Murao, M. Aziz, H. Wang, M. Brenner, P. Wang, Release mechanisms of major DAMPs, *Apoptosis* 26 (3–4) (2021) 152–162.
- [10] Q. Yang, G.W. He, M.J. Underwood, C.M. Yu, Cellular and molecular mechanisms of endothelial ischemia/reperfusion injury: perspectives and implications for postischemic myocardial protection, *Am J Transl Res* 8 (2) (2016) 765–777.
- [11] S. Jacquet, et al., The role of RIP2 in p38 MAPK activation in the stressed heart, *J. Biol. Chem.* 283 (18) (2008) 11964–11971.
- [12] O.H. Lowry, N.J. Rosebrough, A.L. Farr, R.J. Randall, Protein measurement with the Folin phenol reagent, *J. Biol. Chem.* 193 (1) (1951) 265–275.
- [13] W. Songjiang, N. Paiyabhroma, N. Jumroon, A. Jiraviriyakul, N. Nernpermpisooh, P. Seenak, S. Kumphune, S. Thaisakun, N. Phaonakrop, S. Roytrakul, P. Pankhong, Proteomic profiling of early secreted proteins in response to lipopolysaccharide-induced vascular endothelial cell EA.hy 926 injury, *Biomedicines* 11 (11) (2023) 3065.
- [14] S. Tyanova, T. Temu, P. Sinitcyn, A. Carlson, M.Y. Hein, T. Geiger, M. Mann, J. Cox, The Perseus computational platform for comprehensive analysis of (prote) omics data, *Nat. Methods* 13 (9) (2016) 731–740.
- [15] Z. Pang, G. Zhou, J. Ewald, L. Chang, O. Hacariz, N. Basu, J. Xia, Using MetaboAnalyst 5.0 for LC-MS/MS spectra processing, multi-omics integration and covariate adjustment of global metabolomics data, *Nat. Protoc.* 17 (8) (2022) 1735–1761.
- [16] D. Szklarczyk, A. Santos, C. von Mering, L.J. Jensen, P. Bork, M. Kuhn, Stitch 5: augmenting protein-chemical interaction networks with tissue and affinity data, *Nucleic Acids Res.* 4 (44) (2016) D380–D384. D1.
- [17] Y. Lu, Y. Sun, K. Xu, Y. Shao, F. Saaoud, N.W. Snyder, L. Yang, J. Yu, S. Wu, W. Hu, J. Sun, H. Wang, X. Yang, Editorial: endothelial cells as innate immune cells, *Front. Immunol.* 13 (2022) 1035497.
- [18] J. Francisco, Re DP. Del, Inflammation in myocardial ischemia/reperfusion injury: underlying mechanisms and therapeutic potential, *Antioxidants* 12 (11) (2023) 1944.
- [19] T. Gong, L. Liu, W. Jiang, R. Zhou, DAMP-sensing receptors in sterile inflammation and inflammatory diseases, *Nat. Rev. Immunol.* 20 (2) (2020) 95–112.
- [20] B. Tjoe, et al., Coronary microvascular dysfunction: considerations for diagnosis and treatment, *Cleve. Clin. J. Med.* 88 (10) (2021) 561–571.
- [21] T. Scarabelli, et al., Apoptosis of endothelial cells precedes myocyte cell apoptosis in ischemia/reperfusion injury, *Circulation* 104 (3) (2001) 253–256.
- [22] H. Cui, Y. Yang, X. Li, W. Zong, Q. Li, Resveratrol regulates paracrine function of cardiac microvascular endothelial cells under hypoxia/reoxygenation condition, *Pharmazie* 77 (6) (2022) 179–185.
- [23] P. Pintavorn, B.J. Ballermann, TGF-beta and the endothelium during immune injury, *Kidney Int.* 51 (5) (1997) 1401–1412.
- [24] G. Euler, Good and bad sides of TGF beta-signaling in myocardial infarction, *Front. Physiol.* 6 (2015) 66, 2015.
- [25] S. Ramesh, G.M. Wildey, P.H. Howe, Transforming growth factor beta (TGFbeta)-induced apoptosis: the rise & fall of Bim, *Cell Cycle* 8 (1) (2009) 11–17.
- [26] J.A. Kloka, et al., Microvascular leakage as therapeutic target for ischemia and reperfusion injury, *Cells* 12 (10) (2023) 1345, 9.
- [27] P. Kumar, A. Nagarajan, P.D. Uchil, Analysis of cell viability by the lactate dehydrogenase assay, *Cold Spring Harb. Protoc.* 2018 (6) (2018).
- [28] Y.J. Yang, et al., Post-infarction treatment with simvastatin reduces myocardial no-reflow by opening of the KATP channel, *Eur. J. Heart Fail.* 9 (1) (2007) 30–36.
- [29] Y.J. Yang, et al., Post-infarction treatment with simvastatin reduces myocardial no-reflow by opening of the KATP channel, *Eur. J. Heart Fail.* 9 (1) (2007) 30–36.
- [30] K. Hayashi, F. Nikolos, K.S. Chan, Inhibitory DAMPs in immunogenic cell death and its clinical implications, *Cell Stress* 5 (4) (2021) 52–54.
- [31] J.P. Cheng, et al., Caveolae protect endothelial cells from membrane rupture during increased cardiac output, *J. Cell Biol.* 211 (1) (2015) 53–61.
- [32] Z. Chen, et al., Reciprocal regulation of eNOS and caveolin-1 functions in endothelial cells, *Mol. Biol. Cell* 29 (10) (2018) 1190–1202.
- [33] J.A. Troiano, et al., Caveolin-1/Endothelial nitric oxide synthase interaction is reduced in arteries from pregnant spontaneously hypertensive rats, *Front. Physiol.* 12 (2021) 760237.
- [34] B.K. Podesser, S. Hallstrom, Nitric oxide homeostasis as a target for drug additives to cardioplegia, *Br. J. Pharmacol.* 151 (7) (2007) 930–940.
- [35] N. Tran, T. Garcia, M. Aniga, S. Ali, A. Ally, S. Nauli, Endothelial nitric oxide synthase (eNOS) and the cardiovascular system: in physiology and in disease states, *Am J Biomed Sci Res* 15 (2) (2022) 153–177.
- [36] S. Matsushima, H. Tsutsui, J. Sadoshima, Physiological and pathological functions of NADPH oxidases during myocardial ischemia-reperfusion, *Trends Cardiovasc. Med.* 24 (5) (2014) 202–205.
- [37] B.A. Diebold, et al., NOX2 as a target for drug development: indications, possible complications, and progress, *Antioxid Redox Signal* 23 (5) (2015) 375–405.
- [38] S.H. Miao, et al., Increased NOX2 expression in astrocytes leads to eNOS uncoupling through dihydrofolate reductase in endothelial cells after subarachnoid hemorrhage, *Front. Mol. Neurosci.* 16 (2023) 1121944.
- [39] B. Bai, Y. Yang, Q. Wang, M. Li, C. Tian, Y. Liu, L.H.H. Aung, P.F. Li, T. Yu, X.M. Chu, NLRP3 inflammasome in endothelial dysfunction, *Cell Death Dis.* 11 (9) (2020) 776.
- [40] N.R. Jana, M. Tanaka, Gh Wang, N. Nukina, Polyglutamine length-dependent interaction of Hsp 40 and Hsp 70 family chaperones with truncated N-terminal huntingtin: their role in suppression of aggregation and cellular toxicity, *Hum. Mol. Genet.* 9 (13) (2000) 2009–2018.
- [41] S. Wang, W. Yi, Z. Xu, M. Shi, PYCR2 promotes growth and aerobic glycolysis in human liver cancer by regulating the AKT signaling pathway, *Biochem. Biophys. Res. Commun.* 680 (2023) 15–24.
- [42] C. Heiss, A. Rodriguez-Mateos, M. Kelm, Central role of eNOS in the maintenance of endothelial homeostasis, *Antioxid Redox Signal* 22 (14) (2015) 1230–1242.